Supporting Information

Transition-metal phosphite complexes: from one-dimensional chain, two-dimensional sheet, to three-dimensional architecture with unusual magnetic properties

**Jumei Tian,[a] Bo Li,[a,b] Xiaoying Zhang,[a] and Jingping Zhang*[a]**

[a] *Faculty of Chemistry, Northeast Normal University, Changchun 130024, China. E-mail:*
*jpzhang@nenu.edu.cn.*

[b] *Hebei Provincial Key Laboratory of Inorganic Nonmetallic Materials, College of Materials*
Science and Engineering, Hebei United University, Hebei, Tangshan 063009, China.
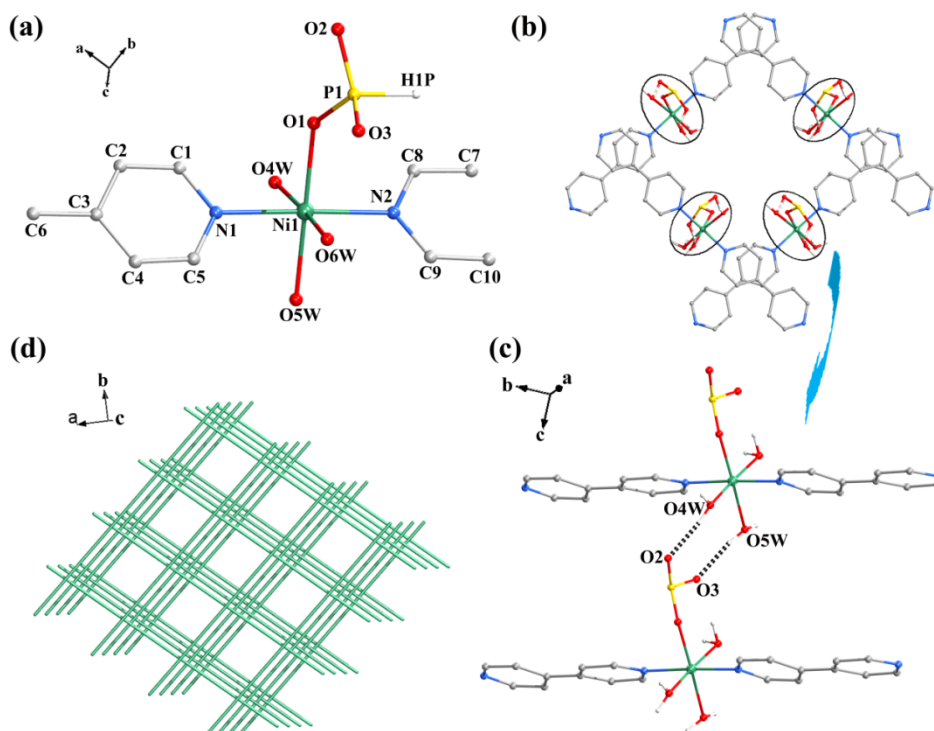
Fig. S1 (a) View of the asymmetric unit and the numbering scheme of complex **1**. The hydrogen atoms are omitted for clarity. (b) View of the 3D supramolecular framework along *c* axis. (c) The hydrogen bonding interaction. (d) The topology of the supermolecular framework. The interstitial water molecules are not shown for clarity.
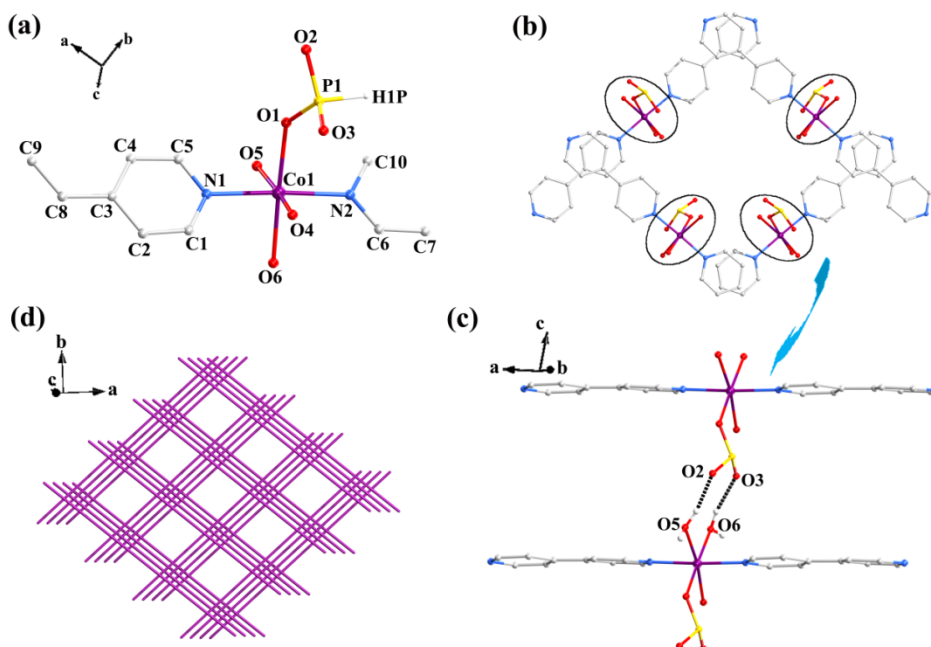

Fig. S2 (a) View of the asymmetric unit and the numbering scheme of complex **2**. The hydrogen atoms are omitted for clarity. (b) View of the 3D supramolecular framework along *c* axis. (c) The hydrogen bonding interaction. (d) The topology of the supermolecular framework. The interstitial water molecules are not shown for clarity.
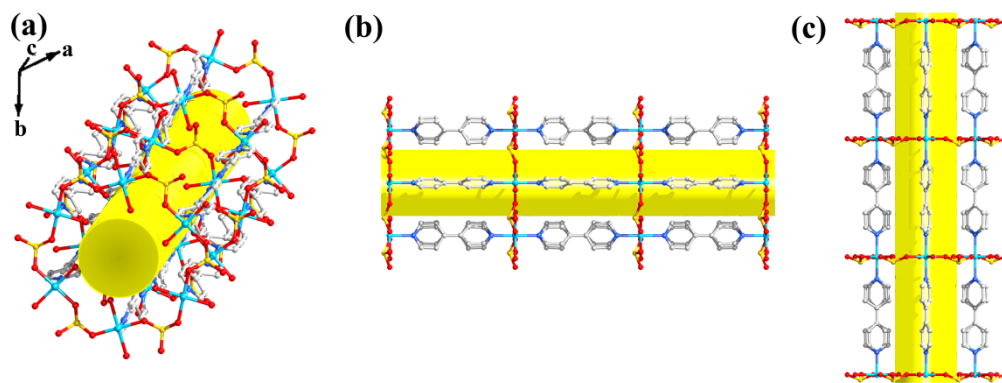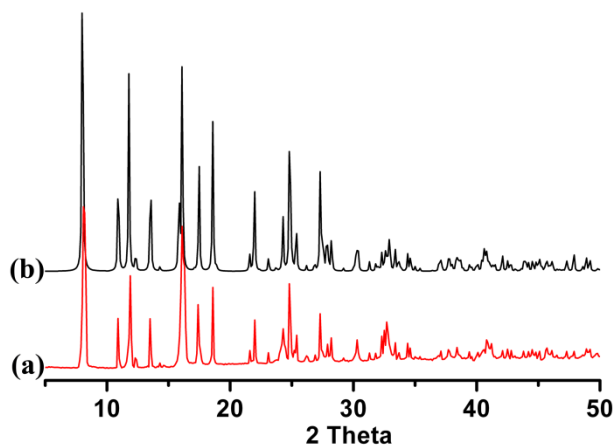
Fig. S3 The 1D channel from different directions for Complex **4** (a) the given direction, (b) *a* axis, (c) *b* axis.
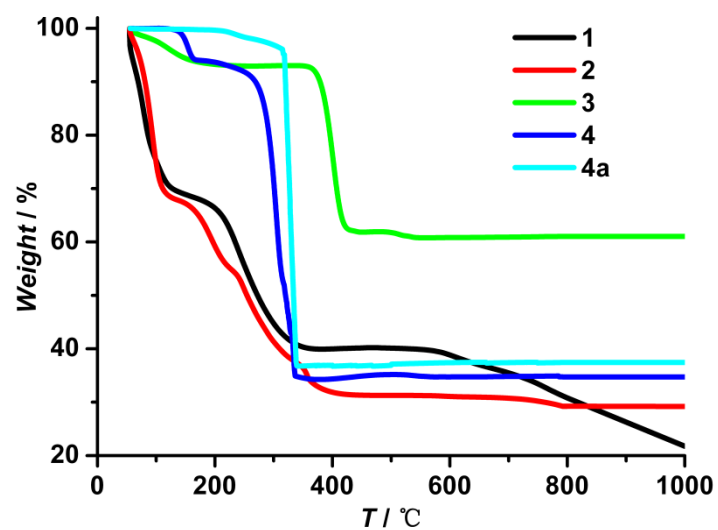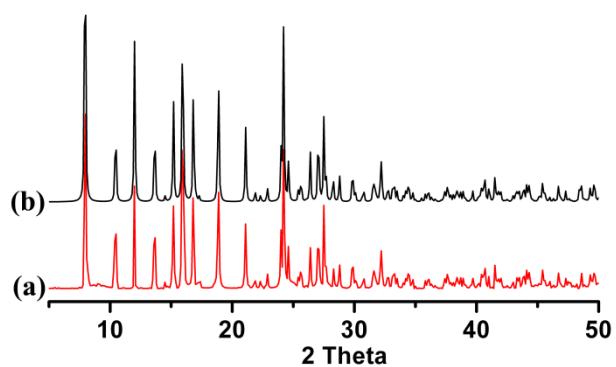

**Fig. S4**. The TGA curves for complexes **1-4** and **4a**.
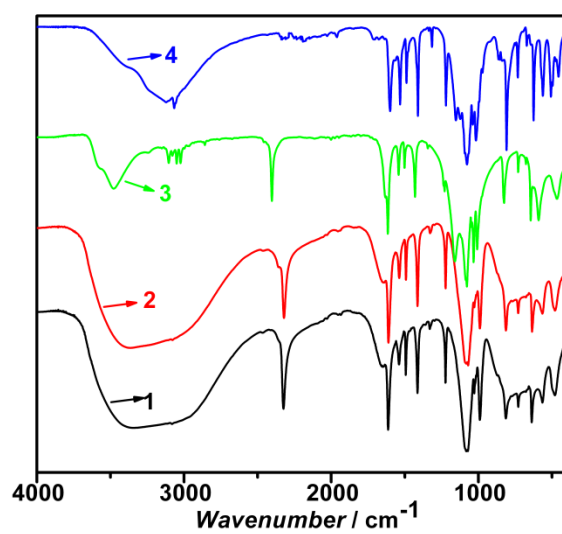
Fig. S5 The IR spectra for complexes **1-4**.

Fig. S6 The Powder X-ray diffraction (PXRD) patterns for complex **1**: (a) the experimental pattern at room temperature; (b) the simulated pattern from single crystal X-ray data.

Fig. S7 The Powder X-ray diffraction (PXRD) patterns for complex **2**: (a) the experimental pattern at room temperature; (b) the simulated pattern from single crystal X-ray data.
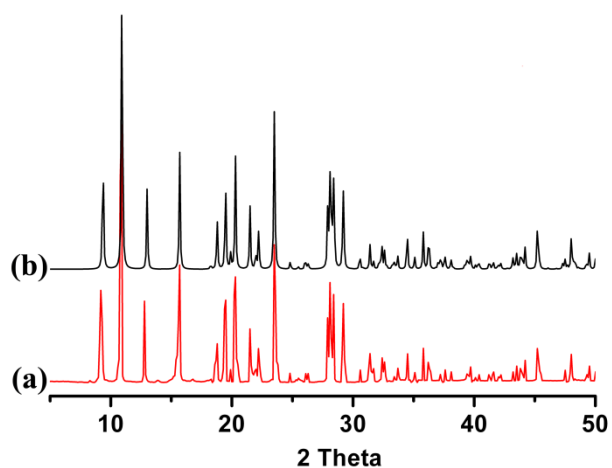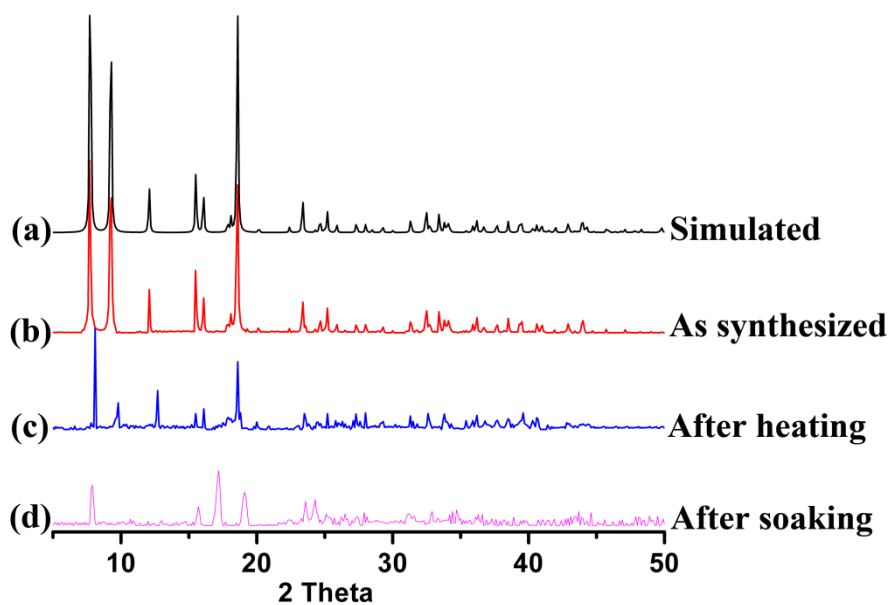

Fig. S8 The Powder X-ray diffraction (PXRD) patterns for complex **3**: (a) the experimental pattern at room temperature; (b) the simulated pattern from single crystal X-ray data.
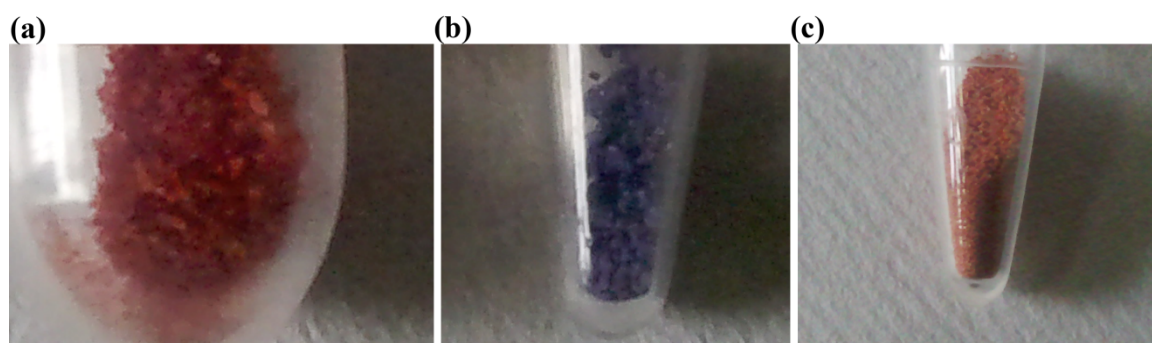
Fig. S9 The Powder X-ray diffraction (PXRD) patterns for complex **4**: (a) the simulated, (b) the as-synthesized sample, (c) the de-solvated **4a**, and (d) the sample after soaking in water for 4 days.

Fig. S10 The color change: (a) **4**, (b) **4a**, (c) the samples after reabsorption of guest.
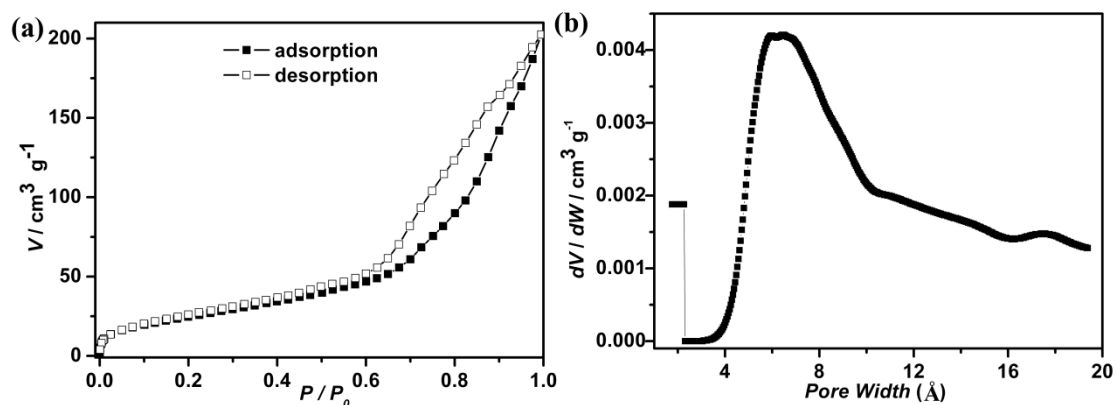
Fig. S11 (a) The N_2-adsorption isotherms at 77 K for **4a.** (b) Pore size distribution estimated from SF-plot model.

Fig. S12 The magnetic data for complex **1**: (a) plots of $\chi_m T$ and χ_m^{-1} versus T at 1000 Oe; (b) the Field dependence of magnetization at 2.0 K.
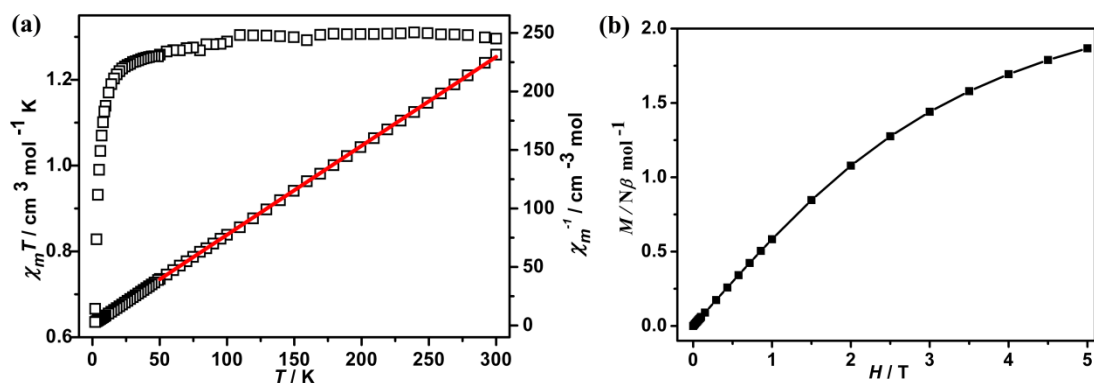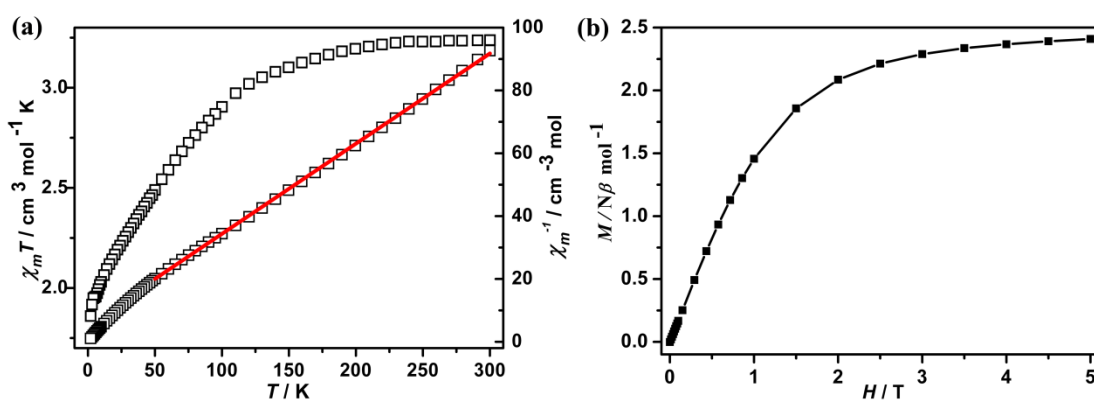

Fig. S13 The magnetic data for complex **2**: (a) plots of $\chi_m T$ and χ_m^{-1} versus T at 1000 Oe; (b) the Field dependence of magnetization at 2.0 K.
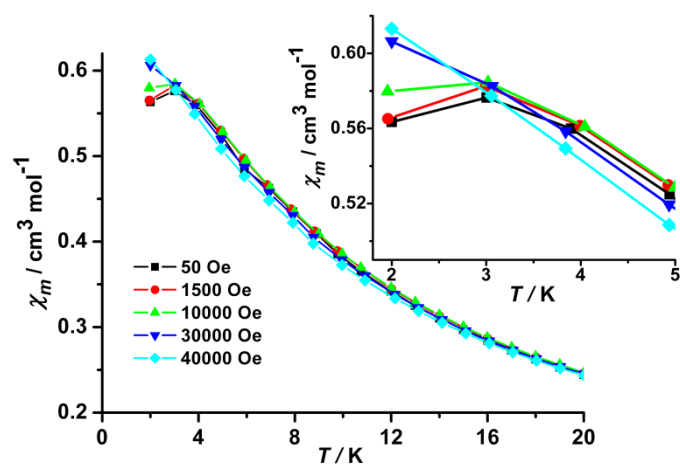
Fig. S14 The χ_m versus T plot in the temperature range 2-20 K for **4** under different external fields. Inset: enlargement of the signal from 2 to 5 K.
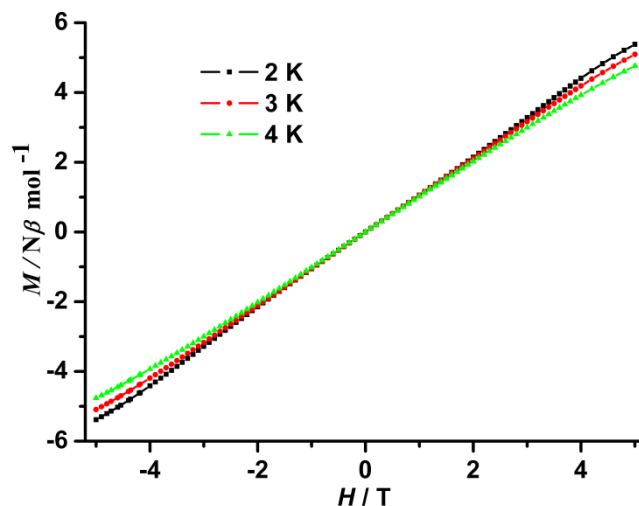
Fig. S15 The displaying no magnetic hysteresis loops at different temperature for **4**.

Fig. S16 The FC and ZFC curve for **4** at applied field strength of 10 Oe.

Fig. S17 The Plots of in-phase and out-of-phase magnetic susceptibilities for **4** under $H_{dc} = 0$ and $H_{ac} = 3.5$.

Fig. S18 The plot of χ_m versus T for **4a.** The red line is the best fitting of Curie-Weiss law.

Fig. S19 The χ_m versus T plot in the temperature range 2-20 K for **4a** under different external fields. Inset: enlargement of the signal from 2 to 8 K.

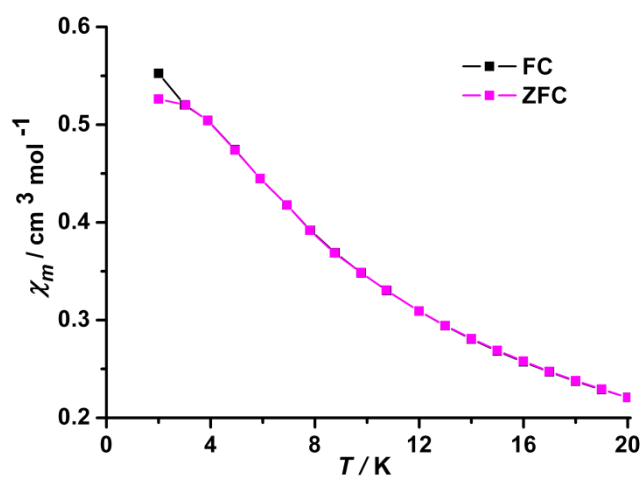**Fig. S20** The displaying no magnetic hysteresis loop for **4a** at 2 K.

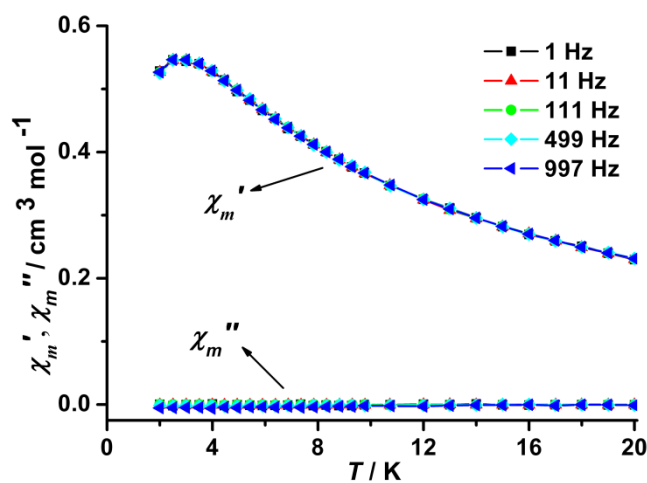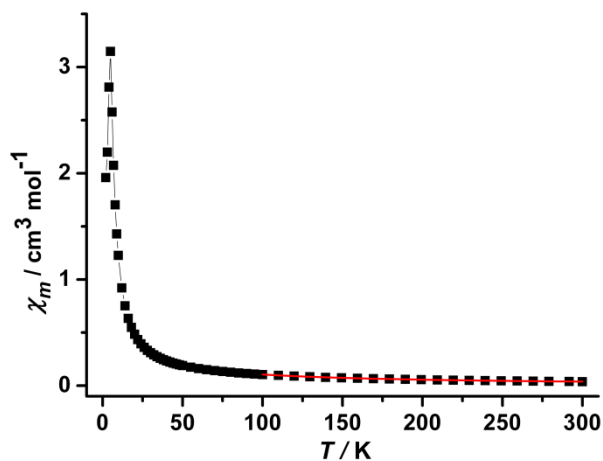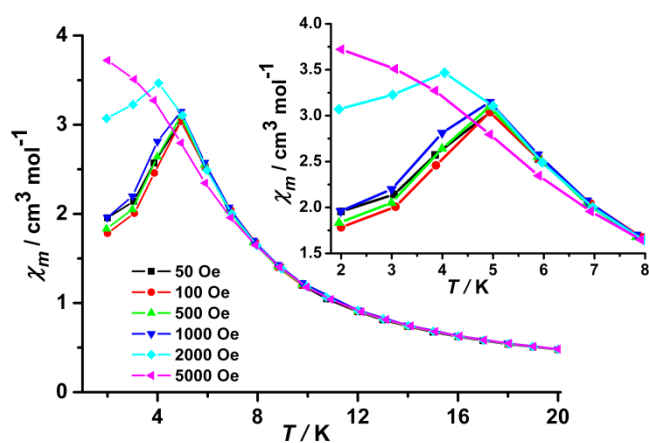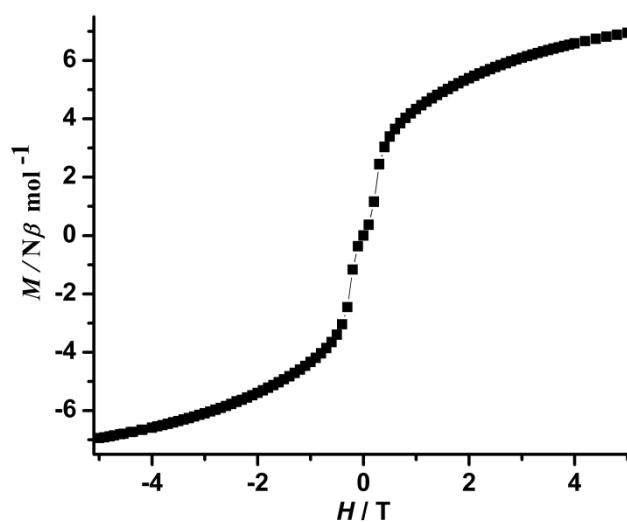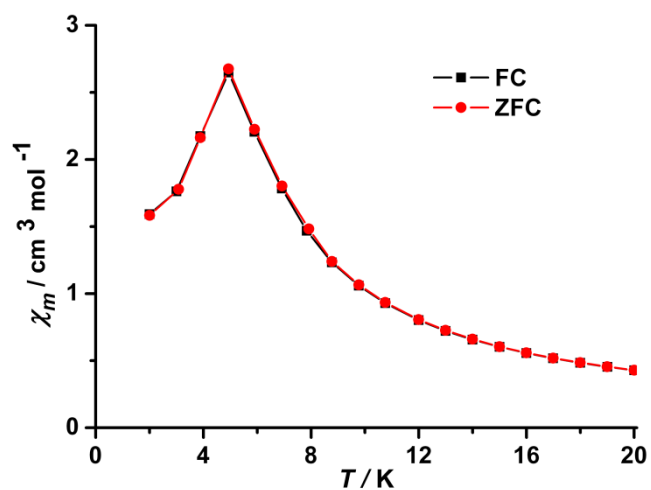**Fig. S21** The FC and ZFC curve for **4a** at applied field strength of 10 Oe.
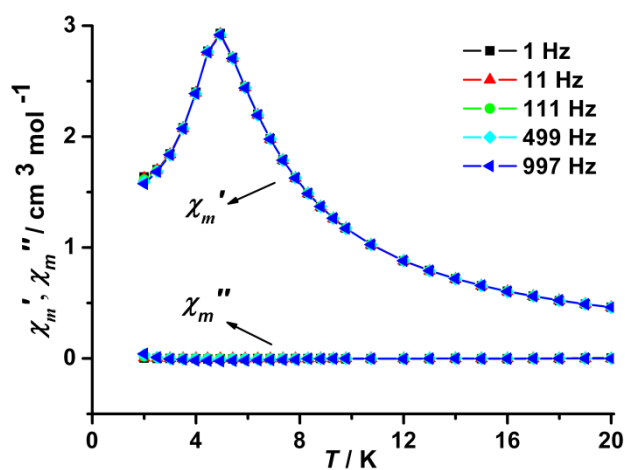

Fig. S22 The Plots of in-phase and out-of-phase magnetic susceptibilities for **4a** under $H_{dc} = 0$ and $H_{ac} = 3.5$.

Table S1. The compounds containing H_3PO_3 and 4, 4'-bpy ligands.

Formula unit	Crystallographic parameters	Dimension	Ref.
$[Ni(HPO_3)(4,4'-bpy)(H_2O)_3]\cdot 4H_2O$ (**1**)	This work in Table S2	1D chain	this work
$[Co_2(HPO_3)_2(4,4'-bpy)_2(H_2O)_6]\cdot 9H_2O$ (**2**)	This work in Table S2	1D chain	this work
$[Zn(HPO_3)(4,4'-bpy)_{0.5}]\cdot H_2O$ (**3**)	This work in Table S2	2D sheet	this work
$[Co_3(PO_3)_2(4,4'-bpy)_3(H_2O)_6]\cdot 3H_2O$ (**4**)	This work in Table S2	3D network	this work
$Co(HPO_3)(4,4'-bpy)(H_2O)$	Monoclinic Cc a=22.477(7) Å b=5.280(1) Å c=10.404(4) Å β=96.08(3)° V=1227.8(7) Å^3	Rectangular grids	[1]
$Zn(HPO_3)(4,4'-bpy)_{0.5}$ (**5**)	Monoclinic $P21/c$ a=9.758(2) Å b=7.449(3) Å c=10.277(2) Å β=100.02(2)° V=735.6(4) Å^3	3D structure	[1]
$[Co(C_{10}H_8N_2)(H_2PO_3)_2]$	Monoclinic $C2/c$ a= 17.2718(6) Å b= 11.4561(4) Å c= 16.9932(5) Å β= 119.014(10)° V=2940.42(17) Å^3	2D layer structure	[2]
$[(C_{10}H_{10}N_2)][V_2^{IV}O_2(HPO_3)_2(H_2PO_3)_2]$	Monoclinic $P21/c$ a= 6.3541(14) Å b= 10.460(2) Å c= 14.769(3) Å β= 90.412(5)° V=981.6(4) Å^3	3D framework	[3]

Table S2. Crystallographic data and structure refinement summary for complexes **1-4**.

	1	2	3	4
formula	$C_{10}H_{23}N_2NiO_{10}P$	$C_{20}H_{48}Co_2N_4O_{21}P_2$	$C_5H_7NO_4PZn$	$C_{30}H_{42}Co_3N_6O_{15}P_2$
fw	421	860.42	241.48	965.43
space group	$C\,2$	$C\,2$	$P\,21/c$	$P\,6/m\,c\,c$
crystal system	Monoclinic	Monoclinic	Monoclinic	Hexagonal
a/Å	16.696(86)	17.189(5)	11.4350(7)	11.0320(5)
b/Å	14.997(79)	14.748(5)	5.2040(2)	11.0320(5)
c/Å	7.400(4)	7.469(5)	16.4787(10)	22.8380(13)
a/°	90	90	90	90
$β$/°	104.42(6)	100.047(5)	124.283(4)	90
$γ$/°	90	90	90	120

V/Å³	1794.5	1864.4(15)	1433.33(13)	2407.1(2)
Z	4	2	4	2
D_c (g.cm⁻³)	1.528	1.500	1.979	1.324
F(000)	848	860	484	977.9
θ range (deg)	1.85 to 27.82	1.83 to 26.02	3.61 to 25.00	4.10 to 27.08
unique reflns (R_{int})	4250 (0.0318)	3690 (0.0415)	1428 (0.0376)	922(0.0414)
R1,[a] wR2[b] (I >2σ(I))	0.0553, 0.1455	0.0541, 0.1285	0.0456, 0.1128	0.0661, 0.1503
R1,[a] wR2[b] (all data)	0.0597, 0.1487	0.0598, 0.1321	0.0539, 0.1224	0.0808, 0.1584
GOF on F^2	1.034	1.053	1.081	1.015

$$^aR = \sum \lVert F_o \rvert - \lvert F_c \rVert / \sum \lvert F_c \rvert .^b wR_2 = \left[\sum w(\lvert F_o \rvert - \lvert F_c \rvert)^2 / \sum w(F_o^2) \right]^{1/2}, w = 1/\sigma(F_o)^2.$$

Table S3. The pH value comparison.

Systems	pH¹	pH²	pH³	pH⁴
1	4.33	4.63	4.33	4.68
2	4.24	4.51	4.46	4.65
3	4.01	4.44	4.11	4.39

Note: [1] the systems without 4-hydroxypyridine; [2] the systems with 4-hydroxypyridine; [3] the systems with 1, 2, 4-triazole; [4] the systems with imidazole.

Table S4. Selected bond lengths (Å) and angles (deg) for **1**.

Bond lengths [Å]			
Ni(1)-O(1)	2.054(4)	Ni(1)-O(4W)	2.067(4)
Ni(1)-O(5W)	2.074(4)	P(1) -O(1)	1.511(4)
Ni(1)-N(2)	2.089(4)	P(1)-O(2)	1.512(5)
Ni(1)-O(6W)	2.092(4)	P(1)-O(3)	1.510(5)
Ni(1)-N(1)	2.084(4)		
Angles [deg]			
O(1)-Ni(1)-O(4W)	88.42(16)	O(1)-Ni(1)-O(5W)	178.01(18)
O(4W)-Ni(1)-O(5W)	89.68(17)	O(1)-Ni(1)-N(1)	91.27(18)
O(4W)-Ni(1)-N(1)	87.98(18)	O(5W)-Ni(1)-N(1)	89.28(18)
O(1)-Ni(1)-N(2)	90.64(17)	O(4W)-Ni(1)-N(2)	91.02(18)
O(5W)-Ni(1)-N(2)	88.78(18)	N(1)-Ni(1)-N(2)	177.8(2)
O(1)-Ni(1)-O(6W)	90.47(17)	O(4W)-Ni(1)-O(6W)	174.73(18)
O(5W)-Ni(1)-O(6W)	91.47(18)	N(1)-Ni(1)-O(6W)	86.89(18)
N(2)-Ni(1)-O(6W)	94.14(19)		

Table S5. Selected bond lengths (Å) and angles (deg) for **2**.

Bond lengths [Å]			
Co(1)-O(1)	2.101(4)	Co(1)-O(4)	2.147(4)
Co(1)-N(1)	2.122(4)	P(1)-O(1)	1.514(4)
Co(1)-O(6)	2.134(4)	P(1)-O(2)	1.531(4)

Co(1)-N(2)	2.130(4)	P(1)-O(3)	1.523(4)
Co(1)-O(5)	2.111(4)		
Angles [deg]			
O(1)-Co(1)-O(5)	87.54(15)	O(1)-Co(1)-N(1)	92.45(16)
O(5)-Co(1)-N(1)	87.79(17)	O(1)-Co(1)-N(2)	91.00(16)
O(5)-Co(1)-N(2)	91.62(16)	N(1)-Co(1)-N(2)	176.47(18)
O(1)-Co(1)-O(6)	177.25(15)	O(5)-Co(1)-O(6)	91.34(16)
N(1)-Co(1)-O(6)	90.02(16)	N(2)-Co(1)-O(6)	86.51(16)
O(1)-Co(1)-O(4)	88.81(15)	O(5)-Co(1)-O(4)	172.38(16)
N(1)-Co(1)-O(4)	85.69(17)	N(2)-Co(1)-O(4)	95.13(17)
O(6)-Co(1)-O(4)	92.59(16)		

Table S6. Selected bond lengths (Å) and angles (deg) for **3.**

Bond lengths [Å]			
Zn(1)-O(3)#1	1.909(3)	P(1)-O(1)	1.500(4)
Zn(1)-O(1)	1.925(4)	P(1)-O(2)	1.518(3)
Zn(1)-O(2)#2	1.927(3)	P(1)-O(3)	1.497(4)
Zn(1)-N(1)	2.047(4)		
Angles [deg]			
O(3)#1-Zn(1)-O(1)	113.90(19)	O(3)#1-Zn(1)-O(2)#2	110.26(16)
O(1)-Zn(1)-O(2)#2	115.51(15)	O(3)#1-Zn(1)-N(1)	108.19(14)
O(1)-Zn(1)-N(1)	101.36(16)	O(2)#2-Zn(1)-N(1)	106.74(15)

Symmetry transformations used to generate equivalent atoms: #1 -x+1, -y+1, -z+2; #2 -x+1, -y, -z+2.

Table S7. Selected bond lengths (Å) and angles (deg) for **4**.

Bond lengths [Å]			
Co(1)-O(1)	2.027(5)	Co(1)-N(1)	2.166(6)
Co(1)-O(2)	2.154(5)	P(1)-O(1)	1.541(5)
Angles [deg]			
O(1)#1-Co(1)-O(2)	87.6(2)	O(1)-Co(1)-O(2)	92.41(19)
O(1)#1-Co(1)-O(1)	180.0	O(2)-Co(1)-O(2)#1	180.0
O(1)-Co(1)-N(1)	90.0	N(1)#1-Co(1)-N(1)	180.0

Symmetry transformations used to generate equivalent atoms: #1 -x+1, -y+1, -z+1.

References

[1] J.-H. Liao, P.-L. Chen, C.-C. Hsu, *J. Phys. Chem. Solids,* **2001**, *62*, 1629.

[2] a) P. Ramaswamy, S. Mandal, N. N. Hegde, R. Prabhu, D. Banerjee, S. V. Bhat, S. Natarajan, *Eur. J. Inorg. Chem.,* **2010**, *2010*, 1829; b) S. Natarajan, S. Mandal, P. Mahata, V. K. Rao, P. Ramaswamy, A. Banerjee, A. K. Paul, K. V. Ramya, *F. R. Orgmet. Chem. Pr. Tri. Sem.,* **2006**, *118*, 525.

[3] X. Jing, L. Zhang, S. Gong, G. Li, M. Bi, Q. Huo, Y. Liu, *Microporous and Mesoporous Materials,* **2008**, *116*, 101.